International Journal of Pharmaceutics 379 (2009) 270–277

Contents lists available at ScienceDirect

International Journal of Pharmaceutics

journal homepage: www.elsevier.com/locate/ijpharm

Pharmaceutical Nanotechnology

Formulation and characterization of polyphenol-loaded lipid nanocapsules

A. Barras[a], A. Mezzetti[b], A. Richard[a], S. Lazzaroni[b,c], S. Roux[a], P. Melnyk[a], D. Betbeder[d], N. Monfilliette-Dupont[a,*]

[a] Equipe de Chimie et MicroNanotechnologies à Visée Thérapeutique, UMR CNRS 8161, Université de Lille 1 et 2, Institut Pasteur de Lille, Institut de Biologie de Lille, 1 rue du Pr. Calmette, 59021 Lille Cedex, France
[b] Laboratoire de Spectrochimie Infrarouge et Raman (LASIR), UMR CNRS 8516, Université des Sciences et Technologies de Lille, Bat C5, Cité Scientifique, 59655 Villeneuve d'Ascq Cedex, France
[c] Department of Organic Chemistry, Pavia, The University, Viale Taramelli 10, 27100 Pavia, Italy
[d] Laboratoire de Physiologie, EA 2689, IMPRT, Université de Lille 2, Faculté de Médecine - Pôle recherche, 1 place de Verdun, 59045 Lille, France

ARTICLE INFO

Article history:
Received 4 February 2009
Received in revised form 27 April 2009
Accepted 25 May 2009
Available online 6 June 2009

Keywords:
Polyphenol
Quercetin
(−)-Epigallocatechin gallate
Lipid nanocapsules

ABSTRACT

The purpose of this study was to design and characterize two flavonoid-loaded lipid nanocapsules (LNC) by applying the phase inversion process, and to enhance their apparent solubility and/or the stability. The flavonoid-loaded LNC were characterized by particle size, encapsulation efficiency, drug leakage rates, stability and spectroscopic studies. It was observed that quercetin-loaded LNC30 (3%) and LNC60 (2%) carried a particle size of 30.3 and 55.1 nm, respectively and significant higher entrapment efficiency. Encapsulation of quercetin (QC) in LNC enabled us to increase its apparent aqueous solubility by a factor of 100. And in view of calculations and results, it seems most probable that QC is arranged at this LNC interface between the oil phase and the hydrophilic polyethylene glycol moieties of the surfactant. In addition, colloidal suspensions proved to be stable in term of encapsulation for at least 10 weeks and QC was not oxidised. With simple chemical modification of (−)-epigallocatechin-3-gallate or (−)-EGCG, it was possible to reach very high encapsulation rates (95%). Thus we obtained stable colloidal suspensions of (−)-EGCG in water over 4 weeks while free (−)-EGCG solubilised in water exhibited 100% degradation within 4 h. The initial problems (solubility and stability) of these flavonoids were resolved thanks to drug-loaded LNC.

1. Introduction

Flavonoids are the most common polyphenols present in plant food. Their common structure is that of a 2-phenyl-1,4-benzopyrone derivative (Fig. 1). Flavonoids comprise more than 6500 compounds and can be categorized into several groups according to their chemical structures (Flavones, flavonols, flavanones, flavan-3-ols, anthocyanidins, isoflavonoids, ...) (Harborne and Williams, 2000). Among flavonoids, quercetin (QC, 3,3′,4′,5,7-pentahydroxyflavone) is the major representative of the flavonol subclass and (−)-epigallocatechin-3-gallate or (−)-EGCG is a flavan-3-ol gallate ester derivative.

QC is ubiquitously distributed in fruits, vegetables, and herbs or related products, e.g. apple, onion, black/green tea and red wine (Pennington, 2002). QC has been extensively investigated for its pharmacological effects that include anti-tumor, anti-inflammatory and antioxidant activities. Nevertheless clinical studies of QC have been limited by its extreme water insolubility requiring dissolution in dimethylsulfoxide (DMSO). However, DMSO is not biologically inert and cases of neurological toxicity or cardiovascular and respiratory problems have been reported (Windrum et al., 2005). Among potential solutions to this problem are two approaches to enhance its solubility: (i) by chemical modification as 3′-(*N*-carboxymethyl)carbamoyl-3,4′,5,7-tetrahydroxyflavone (QC12), a water soluble glycine carbamate prodrug; the relative bioavailability of QC was estimated to be 20–25% QC release from QC12, but QC12 is not orally bioavailable (Mulholland et al., 2001); (ii) by colloidal drug delivery carriers (cyclodextrin and liposome) (Pralhad and Rajendrakumar, 2004; Yuan et al., 2006). Nevertheless, the use of cyclodextrin complex can induce a risk of nephrotoxicity and the use of liposomes is restricted by their limited stability during the storage and administration (Frijlink et al., 1991; Mu and Zhong, 2006).

Another flavonoid particularly studied for its pharmacology properties is (−)-EGCG. This catechin is the most abundant and biologically active compound in green tea and has been shown to have protective properties in several therapeutic fields. However, its benefits on health are limited because (−)-EGCG will be unstable inside the human body, thus leading to reduced bioavailability. Previous studies have shown that poor beneficial activities may be attributed

* Corresponding author. Tel.: +33 3 28 38 50 17.
E-mail address: nicole.dupont@drrt-lille.fr (N. Monfilliette-Dupont).

0378-5173/$ – see front matter © 2009 Published by Elsevier B.V.
doi:10.1016/j.ijpharm.2009.05.054

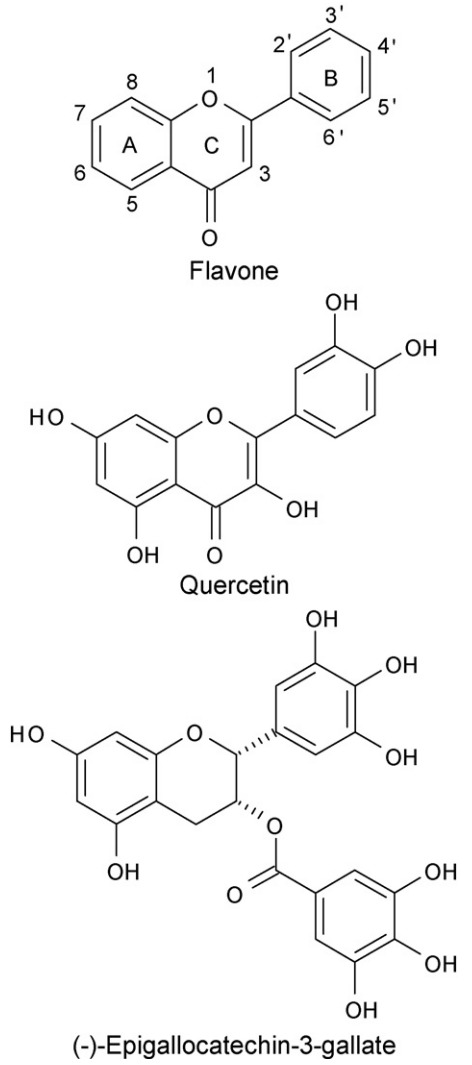

Fig. 1. Chemical structure of flavone (2-phenyl-1,4-benzopyrone), quercetin and (−)-epigallocatechin-3-gallate.

to poor stability of (−)-EGCG in neutral or alkaline solution (Zhu et al., 1997).

For all these reasons, it is necessary to find an alternative delivery method to increase the solubility of QC and stability of (−)-EGCG in order to facilitate their pharmacological effect. The lipid nanocapsules are particularly useful in drug delivery for water-insoluble compounds, or pH sensitive compounds, and may offer a solution to more effective study of the pharmacological properties of flavonoids. Thus, lipid nanocarriers developed by Heurtault et al. (2002) were used for pharmacologic studies of QC and (−)-EGCG. These nanocapsules were prepared according to an organic solvent-free process using the phase inversion method, and consist of an oily liquid triglyceride core surrounded by a tensioactive cohesive interface (which exposes a medium polyethylene glycol chain). The purpose of this study was to design and characterize flavonoid-loaded lipid nanocapsules (LNC) by applying the phase inversion process, and to enhance the apparent solubility or stability of drugs.

2. Materials and methods

2.1. Materials

Quercetin dihydrate (QC) and (−)-epigallocatechin gallate (EGCG) was purchased from Sigma–Aldrich (Saint-Quentin Fallavier, France). Lipid nanocapsules were made of Labrafac™ Lipophile WL 1349 (caprylic/capric triglyceride), Phospholipon® 90G (soybean lecithin at 94–102% of phosphatidylcholine), and Solutol® HS15 (a mixture of free polyethylene glycol 660 and polyethylene glycol 660 hydroxystearate) were generously provided by Gattefosse S.A. (Saint-Priest, France), Phospholipid GmbH (Köln, Germany), and BASF (Ludwigshafen, Germany), respectively. Deionised water was obtained from a Milli-Q plus system (Millipore, Paris, France). All other chemical reagents and solvents were obtained from Prolabo (Fontenay-sous-bois, France) and Carlo Erba (Milan, Italy) and were of analytical grade.

2.2. Synthesis of Pro-EGCG

Synthesis of peracetate-protected EGCG (Pro-EGCG) from (−)-EGCG was done as described (Kohri et al., 2001; Lam et al., 2004). Briefly, commercially available (−)-EGCG was used as a starting material and treated with acetic anhydride and pyridine overnight yielded the desired product in 77% yield.

2.3. Lipid nanocapsule preparation

QC or Pro-EGCG were mixed in Labrafac prior to all the preparation steps by ultrasonication. Thereafter, LNC were prepared at nominal sizes of 30, 60, 110 and 260 nm using a phase inversion method that allows the preparation of very small nanocapsules by thermal manipulation of an oil/water system, as described by Heurtault et al. (2002). Briefly, the oil phase was mixed with the appropriate amounts of Solutol, Phospholipon® 90G, NaCl and distilled water, and heated under magnetic stirring up to 85 °C. The mixture was subjected to 3 temperature cycles from 70 to 90 °C under magnetic stirring. Then, it was cooled to 78 °C, 3.3 mL of distilled cold water (0 °C) were added, and the suspension was stirred at room temperature for another 10 min before further use. The different compositions of the formulations are reported in Table 1. The percentage composition of a drug (QC or Pro-EGCG) is just the mass percentage of oily core (Labrafac + Phospholipon® 90G).

2.4. Characterization of lipid nanocapsules

2.4.1. Lipid nanocapsule size and theoretical calculation

The average diameter and polydispersity index (PI) of the particles were determined by dynamic light scattering (DLS) at 25 °C using a DynaProMS800 (Protein Solutions Inc., Charlottesville, VA). LNC suspensions were diluted at 1/1000 (v/v) in distilled water (filtered over 0.22 μm). Mean results were given for 100 acquisitions, and measurements were performed in triplicate.

The mean theoretical volume of a single nanocapsule was calculated as previously described (Lacoeuille et al., 2007) using mean diameter measurements ($V = 4/3\pi r^3$). Considering a loss of Solutol (10–30%) and all other constituents incorporated into the nanocapsules formulation, the total volume of all nanocapsules (V_T) was estimated by addition of each LNC constituent's volume. The estimated total number (n) of nanocapsules was deduced from previous calculations ($n = V_T/V$) and divided by the volume of the LNC suspen-

Table 1
Composition of the components for the lipid nanocapsules preparation for a total initial mass of 1.26 g.

Density	Labrafac (%)	Solutol (%)	Phospholipon® 90G (%)	NaCl (%)	Water (%)
	0.946 g/mL	1 g/mL	0.97 g/mL		1 g/mL
LNC30	20.0	32.4	3.0	1.7	42.9
LNC60	33.3	19.1	3.0	1.7	42.9
LNC110	40.0	12.4	3.0	1.7	42.9
LNC260	50.0	2.4	3.0	1.7	42.9

Table 2
Calibration curves and linear regression of QC and Pro-EGCG.

Compounds	Retention time (min)	Regression equation[a]	k_{drug}	Linear range (μM)	r^{2b}
QC	12.4	$Y = 18164X$	18,164	10–100	0.995
Pro-EGCG	21.0	$Y = 26345X$	26,345	10–100	0.997

[a] Equation, where Y was the peak area and X was the concentration of compounds.
[b] Correlation coefficient ($n = 7$).

sion (V_S = 4.56 mL) to obtain a number of nanocapsules per milliliter. Labrafac volume used for one formulation and the estimated total number of nanocapsules led to the volume of the core (V_{core}), the mean radius (r_{core}) and surface (S_{core}) of the LNC core ($S_{core} = 4\pi r_{core}^2$). The radius of the shell (r_{shell}) composed by Solutol and Phospholipon® 90G was deduced from the difference $(r) - (r_{core})$.

2.4.2. System chromatographic and calibration curve

Reversed phase-high performance liquid chromatography (RP-HPLC) analyses were performed on a Shimadzu SCL-6A (Shimadzu, Tokyo, Japan). A 5 μm C_4 QS Uptisphere® 300 Å, 250 mm × 4.6 mm column (Interchim, Montluçon, France) was used as the analytical column. The column was heated to 40 °C. Mobile phase was a mixture of eluent A (trifluoroacetic acid 0.05% in H_2O) and eluent B (trifluoroacetic acid 0.05% in CH_3CN/H_2O: 80/20, v/v) at a flow rate of 1 ml/min. The linear gradient was 0% to 100% of eluent B in 30 min and detection was performed at 215 nm.

A 500 μM stock solution of QC or Pro-EGCG was prepared for the calibration curve. Concentrations of 10–500 μM of QC or Pro-EGCG in DMSO were prepared from this stock. Each sample was injected (40 μL) into the RP-HPLC column. Calibration curves were obtained by linear regression of drug concentration (μM) versus the peak area and are shown in Table 2.

2.4.3. Determination of drug loading, drug leakage rates and stability

For determination of QC and Pro-EGCG encapsulation rates, LNC were separated from supernatant using disposable PD-10 desalting columns (Sephadex® G-25 for gel filtration as stationary phase, Amersham Biosciences). A column was stabilized with 25 mL of distilled water. Then 500 μL of a suspension of LNC were deposited on the column, 2 mL of water were added to complete the dead volume of the column, then 4 mL of distilled water eluted and the LNC were collected in this eluant. We measured QC and Pro-EGCG concentrations by RP-HPLC before and after filtration to determine the mean drug payload [drug] by Eq. (1) and the encapsulation efficiency (EE) by Eq. (2).

$$[\text{drug}] = \frac{\text{Area}_{HPLC}}{k_{drug}} \times f_1 \quad (1)$$

$$EE(\%) = \frac{[\text{drug}]_{LNC}}{[\text{drug}]_{TOTAL}} \times f_2 \times 100\% \quad (2)$$

Area_{HPLC}: peak area of drug; k_{drug}: coefficient of a linear regression; f_1: dilution factor to stay in a linear domain of the calibration curve; $[\text{drug}]_{LNC}$: amount of drug loaded in the LNC; $[\text{drug}]_{TOTAL}$: total drug amount in LNC suspension; f_2: dilution factor of gel filtration.

The drug leakage assays of QC and Pro-EGCG were performed at room temperature. The large formulations were used for the drug leakage experiments. At appropriate intervals, 500 μL samples were withdrawn and the amount of QC and Pro-EGCG in the release medium was determined by RP-HPLC similar to the encapsulation rate assay as described below. For determination of LNC stability, we measured the mean diameter and polydispersity of LNC by DLS after filtration.

2.5. Spectroscopic analysis and mass spectrometry

UV–vis spectra were recorded using a Varian Cary-1 spectrophotometer with cells of 1 cm path length. Fluorescence spectra and fluorescence excitation spectra were recorded on a Jobin-Yvon Fluoromax 3 fluorescence spectrophotometer. Fourier Transform-Raman (FT-Raman) spectra were recorded with a Bruker IFS 66 V spectrometer. Radiation of 1064 nm from a Nd:YAG laser was used for the excitation; the spectral resolution was set to 4 cm^{-1}. Spectra results from averaging of 14,000 or 28,000 scans.

Mass spectra were recorded on a Perspective Biosystems Voyager-DE STR, Biospectrometry Workstation MALDI-TOF spectrometer, and measurements were acquired after deposition on a dihydroxybenzoic acid (DHB) matrix.

3. Results and discussion

3.1. Formulation optimization

Previous studies have highlighted the major role of the nature and the ratio of the various excipients on formulation results (Heurtault et al., 2002). Thus, optimised formulation conditions were essential to produce stable particles. The LNC formation was dependent on the excipient proportions (Labrafac, Solutol, Phospholipon® 90G, NaCl and Water). The proportion of NaCl in water was fixed at 1.7% (w/w). The proportion of hydrophilic surfactant (Solutol) had a major influence on the average diameter and the size distribution of the particles, diameter decreasing when its proportion increased. This phenomenon could be explained by the stabilising action of Solutol on the oil-in-water system, greater stability thus allowing the formation of smaller particles (Heurtault et al., 2003). Indeed, the graph (Fig. 2) shows four batches of LNC with various average diameters between 20 and 300 nm (those belonging to the nanometer range, with monodisperse size characteristics (PI < 0.15), and stable upon dilution). The polydispersity of LNC30 and LNC260 was still higher than LNC60 and LNC110. These results show us that we are able to control the LNC size.

3.2. Study of QC-loaded LNC

3.2.1. Preparation and characterization of QC-loaded LNC

By mixing QC with excipients at well-characterised concentrations described above and by applying the phase inversion process (Heurtault et al., 2002); LNC30, LNC60 and LNC110 loaded with

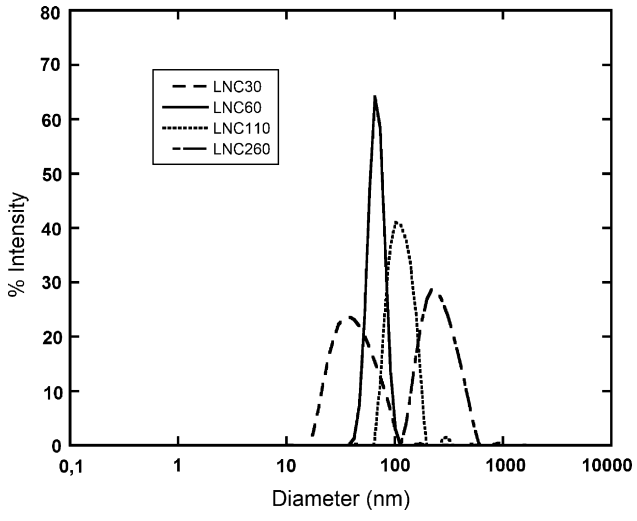

Fig. 2. Particle size distribution of various LNC.

Table 3
Diameter, polydispersity and polydispersity index of different nanocarrier formulation.

	Mean diameter (nm)		Polydispersity (nm)		Polydispersity index	
	Blank	QC (2%)	Blank	QC (2%)	Blank	QC (2%)
LNC30	44.4	30.3	9.1	2.8	0.169	0.037
LNC60	68.0	55.1	5.6	6.2	0.027	0.051
LNC110	114.9	102.0	12.3	6.7	0.046	0.017

QC were obtained. In our study, LNC loaded with 2% QC were monodispersed and presented a slightly narrower size with low polydispersity (PI < 0.05) compared with blank LNC (Table 3). For formulations no significant differences were found between blank and drug-loaded formulations in terms of the particle diameter and their size distribution. Moreover, its stability was also confirmed through the heat cycles required to produce QC-loaded LNC with more than 99% of the drug remaining intact.

3.2.2. Maximal encapsulation efficiency of QC-loaded LNC

To investigate the influence of mass percentage of oily core (i.e. LNC size) on QC entrapment efficiency, different formulations (LNC30, LNC60 and LNC110) were prepared with different amounts of QC (1–4%). Results listed in Table 4 show the maximum amount of QC to be entrapped in LNC30 and LNC60 was around 5 mM. The water solubility of QC is normally 50 μM, so here we have increased the apparent solubility of QC by a factor of 100. This leads to the assumption that LNC could enhance the solubility of certain poorly soluble drugs but to a maximum limit after which any increase in the drug concentration leads to its precipitation (4% QC-loaded LNC30 and 2% QC-loaded LNC110). Furthermore, the general trend for nanoparticles of similar composition is that increasing size translates into more rapid up-take by the reticuloendothelial system. These data suggest that lipid nanocapsules should be small enough, preferably <100 nm (Drummond et al., 1999).

Results listed in Table 4 show also that LNC30 has significant higher entrapment efficiency than other LNC. This could be due to the poor solubility of QC in the oily core. Furthermore, QC shows the deepest interaction with membranes; the ease of this flavonoid to modify the ordered structure of the lipidic bilayer probably depends on its ability to assume a planar conformation (Saija et al., 1995). Thus, one can speculate that, also depending on their liposolubility, there is a relationship between flavonoid interaction with model membranes and formation of flavonoid–phospholipid complexes. To verify this hypothesis, we show in the following calculation in Table 5 that the total area of LNC is inversely proportional to the radius (the mass of LNC was maintained constant). Hydrodynamic diameter size measurements allowed us to determine physical characteristics such as radius, surface and volume of the LNC. Thus, we show that by increasing the nanocapsules' diameter (LNC30, LNC60 and LNC110), we increase the total volume of the oily core (2.66×10^{20}, 4.44×10^{20} and 5.33×10^{20} nm^3, respectively). Conversely, the total surface of the oily core decreases (7.02×10^{19}, 5.56×10^{19} and 3.42×10^{19} nm^2, respectively. Consequently, the graph (Fig. 3) makes it possible to show a correlation between maximal encapsulation of QC and the total surface of the oily core. In view of these calculations and the results, it seems probable that QC is arranged at this LNC interface between the oil phase and the hydrophilic polyethylene glycol moieties of the surfactant, and that its solubility is partial in the Labrafac.

Table 4
Effect of LNC size on the encapsulation efficiency of QC.

	QC (%)	$[QC]_{TOTAL}$ (mM)	$[QC]_{LNC} \times f_2$ (mM)	EE (%)
LNC30	**3**	**5.16**	**5.15**	**99**
	4	6.97	4.53	65
LNC60	**1**	**3.72**	**3.80**	**102**
	2	**6.65**	**5.05**	**76**
LNC110	1	2.79	2.92	104
	2	5.49	2.49	45

Optimal formulations are in bold.

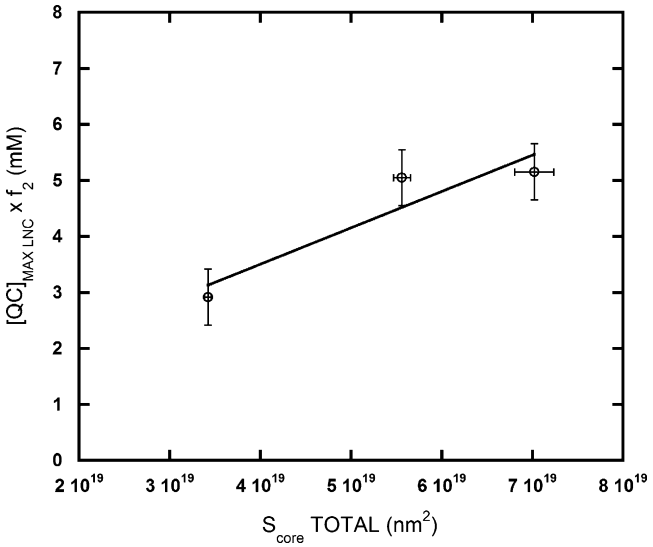

Fig. 3. Correlation of total surface (core) with QC concentration in LNC.

3.2.3. Spectroscopic analysis

UV–vis spectra for 2% QC-loaded LNC60 are shown in Fig. 4. As it can be observed, an intense band is observed at ~375 nm, mainly associated with a HOMO–LUMO transition (Cornard et al., 1997). The origin on the weak shoulder present at ~415–420 nm is not clear up to now, even though it seems to be somehow associated to QC because it is absent (as the 375 nm band) from empty LNC60 particles (see inset in Fig. 4). In order to get some more insight on the molecular environment surrounding the QC molecule, we have recorded spectra of QC in solvents that could somehow mimic the possible molecular environment in the LNC; the rationale for such approach is the fact the molecular environment surrounding

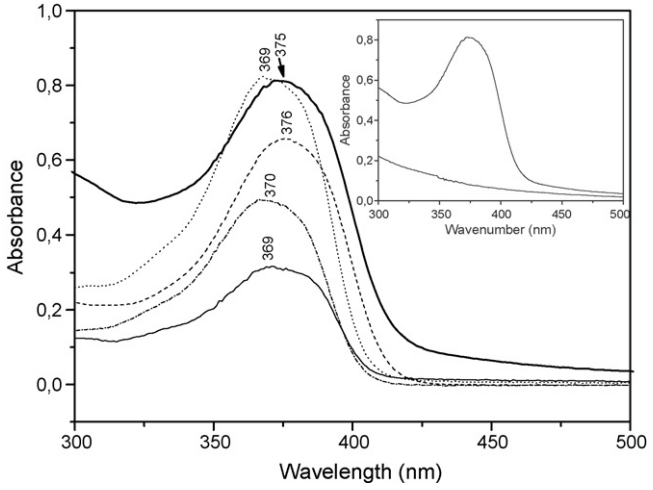

Fig. 4. UV–vis absorption spectra of QC in different conditions. Thick continuous line: absorption spectrum of 2% QC-loaded LNC60 (2.9×10^{-5} M); dotted line: QC in ether (1.3×10^{-5} M); dash-dotted line: QC in ethyl acetate (1.3×10^{-5} M); dashed line: QC (4.3×10^{-5} M) and Phospholipon® 90G (2.1×10^{-4} M) in ethyl acetate; continuous line: QC in Labrafac™ Lipophile WL 1349 (1.3×10^{-5} M). *Inset*: Comparison between UV–vis spectra of QC-loaded and empty LNC60.

Table 5
Physico-chemical characteristics of LNC constituents and nanocapsules.

	LNC30	LNC60	LNC110
V (nm^3)	14,609	87,590	555,974
V_T (nm^3)	$6.31 \times 10^{20} \pm 5.77 \times 10^{19}$	$6.75 \times 10^{20} \pm 3.39 \times 10^{19}$	$6.96 \times 10^{20} \pm 2.21 \times 10^{19}$
n	$4.32 \times 10^{16} \pm 3.95 \times 10^{15}$	$7.70 \times 10^{15} \pm 3.88 \times 10^{14}$	$1.25 \times 10^{15} \pm 3.97 \times 10^{13}$
V_{core} (nm^3)	6187 ± 565	57716 ± 2904	425531 ± 13501
r_{core} (nm)	11.38 ± 0.35	23.97 ± 0.40	46.66 ± 0.49
S_{core} (nm^2)	1629 ± 99	7221 ± 242	27358 ± 579
$V_{core\ TOTAL}$ (nm^3)	2.66×10^{20}	4.44×10^{20}	5.33×10^{20}
$S_{core\ TOTAL}$ (nm^2)	$7.02 \times 10^{19} \pm 2.14 \times 10^{18}$	$5.56 \times 10^{19} \pm 9.32 \times 10^{17}$	$3.42 \times 10^{19} \pm 3.62 \times 10^{17}$
r_{shell} (nm)	3.78 ± 0.35	3.58 ± 0.40	4.35 ± 0.49

a molecule can influence the position and the shape of a given absorption band. We choose (i) Labrafac™ Lipophile WL 1349 (caprylic/capric triglyceride) as a solvent to mimic the core of the LNC; (ii) ethyl ether as a solvent to mimic the PEG environment; (iii) ethyl acetate and (iv) a solution of lecithin (Phospholipon® 90G) in ethyl acetate as two different model solvents to mimic the interface between oil phase and the hydrophilic polyethylene glycol phase, where the head groups of lecithin molecules are present. As observed in Fig. 4, the UV–vis spectrum for the solution of QC in the lecithin/ethyl acetate mixture best reproduces the position and shape of the ~375 nm absorption peak of QC and (partially also) the weak shoulder at ~415–420 nm compared with the other solutions tested. This suggests that the molecular environment of QC in LNC particles is made up of esteric C=O moieties and lecithin headgroups.

As it is known that the molecular environment can also influence the emission properties of QC (Sentchouk and Bondaryuk, 2007), we also recorded the fluorescence spectrum of 2% QC-loaded LNC60, shown in Fig. 5. Excitation at 370 nm gave an emission peak at ~550 nm; as may be expected, a similar peak is absent in empty LNC (Fig. 5, lower trace) so that contributions from any fluorescent impurity can be excluded. It is interesting to note that the excitation spectra for QC-loaded LNC recorded at λ_{em} = 550 nm differs significantly from the absorption spectrum of QC; no peak is observed at 370 nm, and a positive peak is observed at ~415 nm (see inset in Fig. 5). Interestingly, this peak is placed in correspondence of the shoulder observed in the UV–vis absorption spectrum. Recently, similar behaviour (UV–vis spectrum showing a weak shoulder at higher wavelength compared to the most red-shifted absorption peak) has been reported for another flavonol, 3-hydroxyflavone (3HF) (Protti et al., 2008a,b; Mandal and Samanta, 2003) in some organic solvents. This behaviour was attributed to anion formation due to deprotonation of the 3-OH moiety of 3HF; the mechanism leading to this deprotonation was rationalized in terms of hydrogen bonding donating (HBD) acidity or hydrogen bonding accepting (HBA) basicity of the molecules in the surrounding environment, using the HBD/HBA scale of Kamlet-Taft (Reichardt, 1988). As it has been proposed that in QC the most acid proton belongs to the 3-OH moiety (Kadykova et al., 1993), as a working hypothesis it can be argued that a similar phenomenon to that reported in 3HF also occurs for QC. Thus, observation of the 550 nm fluorescence peak can be taken as a possible indication of QC anion formation, which again would point towards QC localization at the interface between the oil phase and the hydrophilic polyethylene glycol phase. The carbonyl moieties and/or the $(RO)_2PO_2^-$ moiety of lecithin could act as HBA towards the 3-OH of QC to give a hydrogen-bond "complex". Formation of such H-bond complex would be a first step to allow subsequent partial QC anion formation, as observed for 3HF (Protti et al., 2008a).

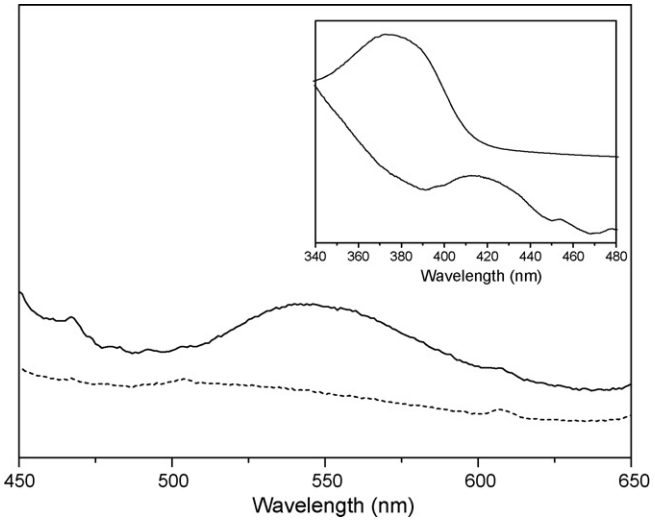

Fig. 5. Fluorescence spectra of 2% QC-loaded LNC60 (continuous line) and empty LNC60 (dashed line). λ_{exc} = 370 nm. *Inset*: Comparison between excitation spectrum (λ_{em} = 550 nm; lower trace) and absorption spectrum (upper trace) for QC-loaded LNC60 nanoparticles.

The spectroscopic analysis was completed by a series of FT-Raman spectra on empty and 2% QC-loaded LNC60 to get some more information on the intermolecular interactions between QC and the different components of LNC and therefore on QC localization. A detailed description on these spectra is beyond the scope of this paper; nevertheless, some clear differences between the two Raman spectra can be easily visualized. As shown in Fig. 6, the spectrum of QC-loaded LNC has clearly visible peaks at 1654, 1626, 1615 and 1573 cm^{-1} given by QC vibrations (Teslova et al., 2007), whereas such peaks are absent in the spectrum for empty LNC. A shoulder at 1321 cm^{-1} is also visible and can be attributed to a QC vibrational mode (Teslova et al., 2007). It is noteworthy that no appreciable changes are observed in the position of the bands given by the components of the LNC, suggesting that no major changes in the architecture of the LNC are taking place.

Molecular vibrations depend on the environment surrounding the molecule; relying on the assignments of bands for QC (Teslova et al., 2007) it is possible to get more information on how QC interacts with neighboring molecules. Indeed, the exact position of a given vibrational band is sensitive to several factors, one of the most important being the presence of hydrogen bonds where atoms involved in the vibrational mode responsible for the band act as donors or acceptors (Silverstein and Webster, 1998). For QC, it becomes difficult to rationalize precisely how different hydrogen bonds contribute to the position of a given Raman band, because a detailed quantum chemical analysis has shown that almost all its bands are given by vibrational modes where several chemical bonds (including bonds capable of accept and donate hydrogen bonds) are involved (Teslova et al., 2007). This is particularly true for the case for the four QC bands visible in the FT-Raman spectrum of QC-loaded LNC (Teslova et al., 2007). Nevertheless, a direct band-for-band comparison of QC spectra in

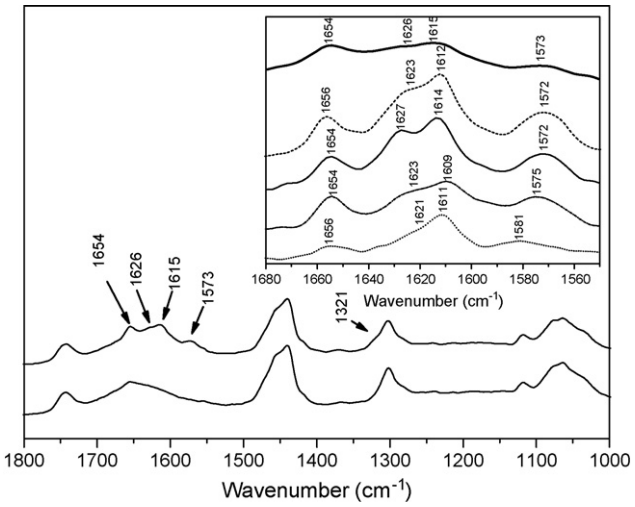

Fig. 6. FT-Raman spectra of 2% QC-loaded LNC60 (1.2×10^{-3} M) (continuous line, upper trace) and empty LNC60 (continuous line, lower trace). *Inset*: Comparison in the 1680–1550 cm^{-1} region between FT-Raman spectrum of QC-loaded LNC60 (continuous thick line) and FT-Raman spectra of QC in different solvents (spectra were obtained after subtraction of the solvent). Dashed line: QC in ether (1.65×10^{-3} M); continuous thin line: QC in ethyl acetate (1.65×10^{-3} M); dash-dotted line: QC (1.15×10^{-3} M) and Phospholipon® 90G (5.75×10^{-3} M) in ethyl acetate (in this case, the spectrum of the solution of Phospholipon® 90G in ethyl acetate was subtracted); dotted line: QC in Labrafac™ Lipophile WL 1349 (4×10^{-4} M).

different solvents of known physicochemical properties (especially their capability to donate or accept hydrogen bonds) should provide information on the molecular environment surrounding QC in the LNC, and is similar to the approach used for the UV–vis experiments, the choice of the solvents being made in order to try to reproduce the different possible molecular environments for the QC molecule in the LNC. As can be seen from the inset in Fig. 6, the QC solution in ethyl acetate is the one that provides a series of peaks at 1654, 1627, 1614, and 1572 cm^{-1} that most closely match (within ± 1 cm^{-1}) those observed in QC-loaded LNC. The solution of QC in ethyl acetate in presence of lecithin shows peaks at 1654, 1623, 1609 and 1575 cm^{-1}; therefore, it does not provide a good match for three (over four) bands, meaning the probably QC interaction with lecithin inside LNC is different from the QC–lecithin interaction taking place in ethyl acetate solutions. The solution of QC in ethyl ether gives a good match only for the 1572 cm^{-1} band, the other ones being at 1656, 1623 (shoulder), 1612 cm^{-1}, i.e. with a up- or down-shift of 2–4 cm^{-1}. The solution of QC in Labrafac™ Lipophile WL 1349 gave peaks for QC at 1656, 1621 (shoulder), 1611 and 1581 cm^{-1}, all the peaks lying therefore at different positions compared to the QC peaks in QC-loaded LNC (with the most pronounced effect for the 1581 cm^{-1} peak, which is upshifted 8 cm^{-1} compared to QC in LNC). It should be noticed that the strong solvent effect on QC Raman peak positions is confirmed by the comparison with literature data for QC in methanol solution, where the above-mentioned bands absorb at 1656, 1627, 1613 and 1577 cm^{-1} (Cornard et al., 1997).

Taking all the FT-Raman results together, it is clear that the QC solution in ethyl acetate is the one that most precisely reproduces the peaks observed in QC-loaded LNC. This suggests that QC inside LNC interacts quite strongly with the esteric C=O moieties of lecithin and polyethylene glycol 660 hydroxystearate.

3.2.4. Drug leakage rates and stability of QC-loaded LNC

Results for the leakage of QC from 2.5% QC-loaded LNC30 and 1.5% QC-loaded LNC60 are shown in Fig. 7. The encapsulation rate of QC-loaded LNC30 did not change over time (originally 67% and 64% after 77 days). Consequently there is no leakage of QC from LNC30 over time. LNC60 allowed a greater initial encapsulation rate of QC (81%), but after 76 days, the encapsulation rate fell to 66%, representing a 15% leakage. The LNC60 exhibited a slight leakage of QC during the time compared with LNC30 but a higher encapsulation rate. Parallel studies of the leakage of QC-loaded LNC60 in various solutions with different ionic strength do not show significant leakage after 4 days (data not shown). This suggests that QC is regardless sufficiently buried in LNC.

The diameter of LNC is a crucial factor of stability. Indeed, if they deteriorate, the diameters change. Result from this study show that over time, mean diameters of LNC30 and LNC60 did not vary. The average diameter of LNC30 and LNC60 were 27 and 54 nm, respectively. Similarly, polydispersities remained constant; hence the formulations are considered stable under the conditions studied here.

3.3. Study of Pro-EGCG-loaded LNC

3.3.1. Preparation and characterization of Pro-EGCG-loaded LNC

Owing to the high solubility of EGCG in water, it was not possible to obtain effective encapsulation of this compound (data not shown). One approach to reduce the water solubility of EGCG is to hide the hydroxyl groups, and Lam et al. (2004) used this strategy to enhance the stability of EGCG. Here, we introduced peracetate protection groups onto the reactive hydroxyls of EGCG (Kohri et al., 2001) hypothesising that synthesis of this Pro-EGCG (a prodrug form of EGCG) would improve encapsulation. Results show that LNC60 loaded with 1% Pro-EGCG were monodispersed, presented a narrow size (57 nm) with low polydispersity (PI < 0.05) and had quantitative entrapment efficiency. Moreover, its stability was also confirmed through the heat cycles required to produce Pro-EGCG-loaded LNC with more than 99% of the drug remaining intact.

3.3.2. Maximal encapsulation efficiency of Pro-EGCG-loaded LNC

In order to find the optimum entrapment efficiency, LNC60 were prepared with different amounts of Pro-EGCG (1%, 1.5% and 2%). Results showed the encapsulation rate of 1.5% Pro-EGCG-loaded LNC60 was 95% and the maximum amount of Pro-EGCG to be entrapped in LNC was determined to be 1.62 mM for these LNC.

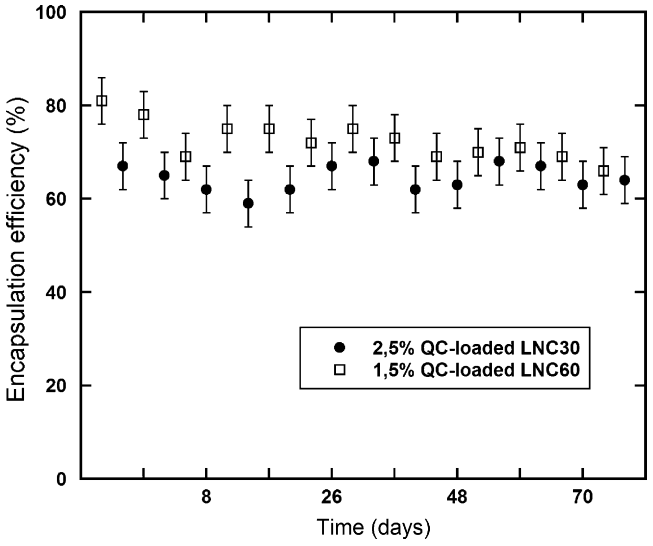

Fig. 7. Drug leakage rates of QC-loaded LNC.

Table 6
Analysis of partially desacetylated Pro-EGCG-loaded LNC60 by RP-HPLC (at 215 nm).

Peaks	Retention times (min)	*m/z* values (observed)	Attributions	*m/z* values (calculated)
1	13.62	585.5	$[Pro\text{-}EGCG - 5Ac + H]^+$	585.12
2	14.07	585.4	$[Pro\text{-}EGCG - 5Ac + H]^+$	585.12
3	14.50	585.4	$[Pro\text{-}EGCG - 5Ac + H]^+$	585.12
4	14.96	585.4	$[Pro\text{-}EGCG - 5Ac + H]^+$	585.12
5	15.82	691.2	$[Pro\text{-}EGCG - 3Ac + Na]^+$	691.13
6	16.74	733.2	$[Pro\text{-}EGCG - 2Ac + Na]^+$	733.15
7	17.60	733.2	$[Pro\text{-}EGCG - 2Ac + Na]^+$	733.15
8	17.82	775.3	$[Pro\text{-}EGCG - 1Ac + Na]^+$	775.15
9	18.74	817.3	$[Pro\text{-}EGCG + Na]^+$	817.15

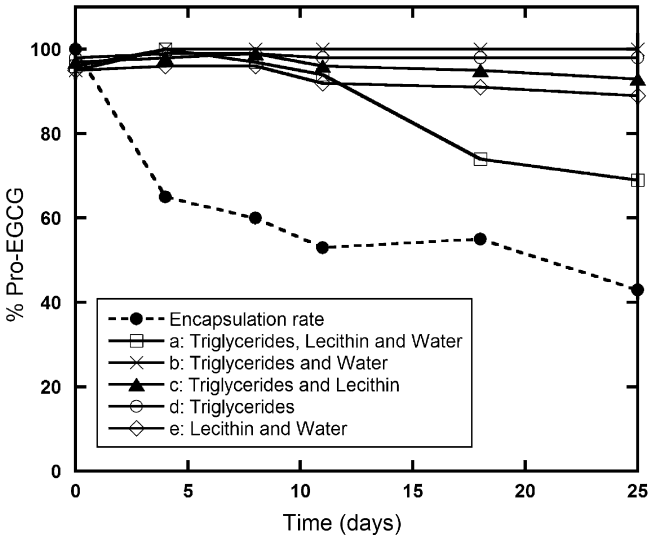

Fig. 8. Drug leakage rates of 1% Pro-EGCG-loaded LNC60 and desacetylation of Pro-EGCG in various mixtures.

3.3.3. Drug leakage rates and stability of Pro-EGCG-loaded LNC

Results for the leakage of 1% Pro-EGCG-loaded LNC60 are shown in Fig. 8. The encapsulation rate of Pro-EGCG-loaded LNC60 decreased over time, being initially 100% and after 8 days decreasing to 60%. However, this reduction of the encapsulation rate is not due to the leakage of this compound from the nanocapsules, but instead to the partial desacetylation of Pro-EGCG inside the LNC (Table 6). Despite a partial desacetylation (50% of initial Pro-EGCG), the amount of EGCG remains constant around 1.13 ± 0.18 mM over 25 days inside the LNC. A parallel study of the degradation of Pro-EGCG in various constituents of nanocapsules and mixtures (triglycerides, lecithin, and water) shows a very low desacetylation of this compound (less than 30% for mixture a, and less than 10% for mixtures b–e after 25 days). This suggests that this process would be linked to the phenomenon of confinement.

Mean diameters of LNC60 did not vary and the average diameter was 57 nm. Similarly, polydispersities remained constant; hence the formulations are considered stable under the conditions described here.

4. Conclusion

The lipid nanocapsules (LNC) studied here can be used as flavonoid delivery carriers. The preparation method used provided flavonoid-loaded nanocapsules in a size range from 20 to 110 nm with a very low particle size polydispersity index. In the case of QC, high drug loading into the LNC can increase its apparent aqueous solubility by a factor of 100. It was also found that the stability of (−)-EGCG was prolonged over a significant period, which could permit the delivery of (−)-EGCG with little or no initial drug loss. These improvements may give new hope for the efficient delivery of these active drugs in different therapeutic areas.

Acknowledgments

This work was financially supported by “La Ligue Nord Pas-de-Calais”, “Le Cancéropôle Nord-Ouest”, “L’Université de Lille 2” and “La région Nord Pas-de-Calais”. S.L. acknowledges “Collège Doctoral Européen Nord Pas-de-Calais” for partial funding of its stay in Lille. We gratefully acknowledge CNRS, Université de Lille 2, Université de Lille 1, Institut Pasteur de Lille for logistical support, Hervé Drobecq for MALDI-TOF acquisitions, Gérard Montagne for NMR acquisitions and Michael Howsam for proof reading.

References

Cornard, J.P., Merlin, J.C., Boudet, A.C., Vrielynk, L., 1997. Structural studies of quercetin by vibrational and electronic spectroscopies combined with semiempirical calculations. Biospectroscopy 3, 183–193.
Drummond, D.C., Meyer, O., Hong, K., Kirpotin, D.B., Papahadjopoulos, D., 1999. Optimizing liposomes for delivery of chemotherapeutic agents to solid tumors. Pharmacol. Rev. 51, 691–743.
Frijlink, H.W., Eissens, A.C., Hefting, N.R., Poelstra, K., Lerk, C.F., Meijer, D.K., 1991. The effect of parenterally administered cyclodextrins on cholesterol levels in the rat. Pharm. Res. 8, 9–16.
Harborne, J.B., Williams, C.A., 2000. Advances in flavonoid research since 1992. Phytochemistry 55, 481–504.
Heurtault, B., Saulnier, P., Pech, B., Proust, J.E., Benoit, J.P., 2002. A novel phase inversion-based process for the preparation of lipid nanocarriers. Pharm. Res. 19, 875–880.
Heurtault, B., Saulnier, P., Pech, B., Venier-Julienne, M., Proust, J., Phan-Tan-Luu, R., Benoit, J.P., 2003. The influence of lipid nanocapsule composition on their size distribution. Eur. J. Pharm. Sci. 18, 55–61.
Kadykova, E.L., Gubina, S.M., Pron'kin, A.M., 1993. Studies on the acidic properties of quercetin as a model of natural dyes for cotton. Koksnes Kimija 1–3, 107–111.
Kohri, T., Nanjo, F., Suzuki, M., Seto, R., Matsumoto, N., Yamakawa, M., Hojo, H., Hara, Y., Desai, D., Amin, S., Conaway, C.C., Chung, F.L., 2001. Synthesis of (−)-[4-3H]epigallocatechin gallate and its metabolic fate in rats after intravenous administration. J. Agric. Food Chem. 49, 1042–1048.
Lacoeuille, F., Hindre, F., Moal, F., Roux, J., Passirani, C., Couturier, O., Cales, P., Le Jeune, J.J., Lamprecht, A., Benoit, J.P., 2007. In vivo evaluation of lipid nanocapsules as a promising colloidal carrier for paclitaxel. Int. J. Pharm. 344, 143–149.
Lam, W.H., Kazi, A., Kuhn, D.J., Chow, L.M., Chan, A.S., Dou, Q.P., Chan, T.H., 2004. A potential prodrug for a green tea polyphenol proteasome inhibitor: evaluation of the peracetate ester of (−)-epigallocatechin gallate [(−)-EGCG]. Bioorg. Med. Chem. 12, 5587–5593.
Mandal, P.K., Samanta, A., 2003. Evidence of ground-state proton-transfer reaction of 3-hydroxyflavone in neutral alcoholic solvents. J. Phys. Chem. A 107, 6334–6339.
Mu, X., Zhong, Z., 2006. Preparation and properties of poly(vinyl alcohol)-stabilized liposomes. Int. J. Pharm. 318, 55–61.
Mulholland, P.J., Ferry, D.R., Anderson, D., Hussain, S.A., Young, A.M., Cook, J.E., Hodgkin, E., Seymour, L.W., Kerr, D.J., 2001. Pre-clinical and clinical study of QC12, a water-soluble, pro-drug of quercetin. Ann. Oncol. 12, 245–248.
Pennington, J.A.T., 2002. Food composition databases for bioactive food components. J. Food Compos. Anal. 15, 419–434.
Pralhad, T., Rajendrakumar, K., 2004. Study of freeze-dried quercetin-cyclodextrin binary systems by DSC, FT-IR, X-ray diffraction and SEM analysis. J. Pharm. Biomed. Anal. 34, 333–339.
Protti, S., Mezzetti, A., Cornard, J.P., Lapouge, C., Fagnoni, M., 2008a. Hydrogen bonding properties of DMSO in ground-state formation and optical spectra of 3-hydroxyflavone anion. Chem. Phys. Lett. 467, 88–93.
Protti, S., Mezzetti, A., Lapouge, C., Cornard, J.P., 2008b. Photochemistry of metal complexes of 3-hydroxyflavone: towards a better understanding of the influence of

solar light on the metal-soil organic matter interactions. Photochem. Photobiol. Sci. 7, 109–119.
Reichardt, C., 1988. Solvents and Solvent Effects in Organic Chemistry. VCH, Weinheim, Germany, p. 378.
Saija, A., Scalese, M., Lanza, M., Marzullo, D., Bonina, F., Castelli, F., 1995. Flavonoids as antioxidant agents: Importance of their interaction with biomembranes. Free Radical Biol. Med. 19, 481–486.
Sentchouk, V.V., Bondaryuk, E.V., 2007. Fluorescent analysis of interaction of flavonols with haemoglobin and bovine serum albumin. J. Appl. Spectrosc. 74, 731–737.
Silverstein, R.M., Webster, F.X., 1998. Spectrometric Identification of Organic Compounds, 6th edition. John Wiley & Sons, Inc.
Teslova, T., Corredor, C., Livingstone, R., Spataru, T., Birke, R.L., Lombardi, J.R., Cañamares, M.V., Leona, M., 2007. Raman and surface-enhanced Raman spectra of flavone and several hydroxyl derivatives. J. Raman Spectrosc. 38, 802–818.
Windrum, P., Morris, T.C., Drake, M.B., Niederwieser, D., Ruutu, T., 2005. Variation in dimethyl sulfoxide use in stem cell transplantation: a survey of EBMT centres. Bone Marrow Transplant. 36, 601–603.
Yuan, Z.P., Chen, L.J., Fan, L.Y., Tang, M.H., Yang, G.L., Yang, H.S., Du, X.B., Wang, G.Q., Yao, W.X., Zhao, Q.M., Ye, B., Wang, R., Diao, P., Zhang, W., Wu, H.B., Zhao, X., Wei, Y.Q., 2006. Liposomal quercetin efficiently suppresses growth of solid tumors in murine models. Clin. Cancer Res. 12,3193–3199.
Zhu, Q.Y., Zhang, A., Tsang, D., Huang, Y., Chen, Z.Y., 1997. Stability of green tea catechins. J. Agric. Food Chem. 45, 4624–4628.